Electronic Supplementary Information

Zirconium ion-mediated assembly of single quantum dot-based nanosensor for kinases assay

Yueying Li,[‡,a] Qian Liu,[‡,a] Lin Cui, [‡,a] Wenjing Liu,[‡,b] Jian-Ge Qiu,*[,b] and Chun-yang Zhang*[,a]

[a] College of Chemistry, Chemical Engineering and Materials Science, Collaborative Innovation Center of Functionalized Probes for Chemical Imaging in Universities of Shandong, Key Laboratory of Molecular and Nano Probes, Ministry of Education, Shandong Provincial Key Laboratory of Clean Production of Fine Chemicals, Shandong Normal University, Jinan 250014, China.

[b] Department of Internal Medicine, Affiliated Cancer Hospital of Zhengzhou University, Academy of Medical Sciences, Zhengzhou University, Zhengzhou 450000, China.

* Corresponding author. E-mail: cyzhang@sdnu.edu.cn (C.-y. Zhang), jiangeqiu@zzu.edu.cn (J.G. Qiu).

[‡] These authors contributed equally.

EXPERIMENTAL SECTION

Materials. T4 polynucleotide kinase (PNK), cAMP−dependent protein kinase (PKA), uracil DNA glycosylase (UDG) and adenosine 5′-triphosphate (ATP) were bought from New England Biolabs (Ipswich, MA, USA). The peptide substrate of PKA (its sequence was Cy5-(COOH)-KLRRASL-(NH_2)) was synthesized by Chinese Peptide Company (Hangzhou, China). The DNA substrate of PNK (its sequence was 5'- GTT GAG C-Cy5-3'), capture probe (its sequence was 5'-PO4-TTT TTT TTT T-biotin-3') were synthesized by Sangon Biotech Co., Ltd. (Shanghai, China). Magnesium chloride (MgCl2), sodium chloride (NaCl), bovine serum albumin (BSA), ammonium sulfate ($(NH4)_2SO_4$), forskolin (Fsk), immunoglobulin G (IgG), 3-isobutyl-1-methylxa-nthine (IBMX), N-[2-(p-bromocinnamylamino) ethyl]-5-isoquinolinesulfonamide dihydrochloride (H-89), Brij-35, glycerol, adenosine diphosphate (ADP), zirconyl chloride octahydrate and Tris-HCl were bought from Sigma-Aldrich Company (St. Louis, MO, USA). Ethylenediaminetetraacetic acid (EDTA) was purchased from Solarbio Bioscience & Technology Co. Ltd. (Beijing, China). The 605 nm-emission streptavidin-coated CdSe/ZnS quantum dots (QD) were obtained from Invitrogen Corporation (Carlsbad, CA, USA). Human cervical carcinoma cell line (HeLa cells) was obtained from Cell Bank, Shanghai Institutes for Biological Sciences, Chinese Academy of Sciences (Shanghai, China). Ultrapure water was obtained from a Millipore filtration system (Millipore, Milford, MA).

Assembly of the QD−Capture Probe Nanostructure. The 2.5 nM QD, 150 nM capture probe, 2 μL of 10 × QD buffer (100 mM $(NH_4)_2SO_4$, 1 M Tris-HCl, 30 mM $MgCl_2$, pH 8.0) were incubated in the dark for 20 min at room temperature to obtain the QD−capture probe nanostructures, and they were stored at 4 ℃ for further use.

Assembly of the QD−Zr4+−Cy5 Nanostructure and Fluorescence Measurement. For PKA assay, the stock solution was diluted with the buffer (50% glycerol, 1 mM EDTA, 50 mM NaCl, and 20 mM Tris−HCl, pH 7.5). Then the PKA-catalyzed phosphorylation reaction was performed in 20 μL of solution containing 2.5 μM peptide substrate, 10 μM ATP, 2 μL of 10 × PKA reaction buffer (0.01% Brij-35, 100 mM $MgCl_2$, 500 mM Tris HCl, PH 7.5), and various concentrations of PKA at 37 °C for 2 h, followed by termination at 65 °C for 20 min.

For the construction of QD-Zr^{4+}-Cy5 nanostructure, 20 μL of QD-capture probe nanostructures and 1.8 μL of 1 mM Zr^{4+} were incubated for 1 h at room temperature, followed by incubation with the phosphorylation reaction mixture for 1 h. The fluorescence intensity of reaction products was measured by using FLS-1000 fluorescence spectrometer (Edinburgh Instruments Ltd., Livingston, United Kingdom). The emission spectra in the range of 550 - 750 nm were obtained at the excitation wavelength of 405 nm, with the emission intensities at 608 nm for QDs and at 670 nm for Cy5 were employed for data analysis.

The PNK-catalyzed phosphorylation reaction was carried out in 20 μL of solution containing 2.5 μM DNA substrate (its sequence was 5'-GTT GAG C-Cy5-3'), 0.8 mM ATP, 2 μL of 10 × PNK reaction buffer (700 mM Tris-HCl, 100 mM $MgCl_2$, pH 7.5), various concentration of PNK at 37 °C for 1.5 h. After dephosphorylation, the reaction was terminated at 65 °C for 20 min. The following procedures were same as those of PKA assay described in main text.

Single-Molecule Detection and Data Analysis. Before single-molecule detection, the reaction products were diluted 50-fold with the buffer (10 mM $(NH_4)_2SO_4$, 3 mM $MgCl_2$, 100 mM Tris-HCl, pH 8.0). The 10 μL of samples were put on a coverslip for total internal reflection fluorescence (TIRF) microscopy (Nikon, Ti-E, Japan) imaging. The QDs were excited by a 405-nm laser. A 100×

objective (Nikon, Japan) was employed to collect the photons from QD and Cy5 and a digital CMSO EMCCD camera (Hamamatsu Photonics K. K., Japan) was employed to obtain the images at an exposure time of 500 ms. Image J software was used for data analysis of a region of interest of 500 × 500 pixels. Cy5 counting were obtained by calculating ten frames.

Inhibition of PKA Activity by H-89. For PKA inhibition assay, 1 U/mL PKA was incubated with different concentrations of H-89 in the PKA reaction solution. The measurement of Cy5 counts follows same procedure described above. The relative activity (*RA*) of PKA was calculated based on equation 1.

$$RA = \frac{C_i}{C_t} \times 100\ \% = 10^{(N_i - N_t)/71.63} \times 100\ \% \quad (1)$$

where N_t represents the Cy5 counts in the presence of 1 U/mL PKA, and N_i represents the Cy5 counts in the presence of 1 U/mL PKA + inhibitors. C_i and C_t were obtained according to the linear correlation equation (Fig. 3B), respectively.

$$N_t = 218.79 + 71.63 log_{10} C_t \quad (2)$$

$$N_i = 218.79 + 71.63 log_{10} C_i \quad (3)$$

The IC_{50} value of inhibitor was obtained from the curve-fitting equation (Fig. 4B).

Cell Culture and Drug Treatment for In Vivo PKA assay. The HeLa cells were cultured in Dulbecco's modified Eagle's medium (DMEM) containing 1% penicillin-streptomycin and 10% fetal bovine serum in 5% CO_2 atmosphere at 37 ºC. Prior to stimulation, the culture medium was replaced with a serum-free medium for 4 h. Then intracellular PKA was activated with Fsk /IBMX for 30 min. The cells treated with equal volume of DMSO (1 mL) was used as the negative control. For H-89-induced inhibition assay, Fsk, IBMX, and H-89 were incubated simultaneously for 30 min. After washing with 1×PBS buffer (pH 7.4) for three times, the cells were collected with

trypsinization for the preparation of cellular extracts. The number of cells was measured by using Countstar automated cell counter (IC1000, Wilmington, DE, USA). About 10^6 cells were suspended in 100 μL of RIPA lysis buffer (0.1% SDS, 1% Triton X-100, 1% sodium deoxycholate, 150 mM NaCl, 50 mM Tris, pH 7.4), and incubated on ice for 10 min, followed by sonication. The obtained supernatant was subjected to PKA activity assay. A modified Lowry protein assay kit (C504041, Sangon Biotech, Shanghai, China) was used for the quantification of protein concentration. PKA activity was measured when the concentration of cell lysate was fixed at 200 μg/mL. The procedures for the in vivo PNK assay were described in the supporting information.

PNK inhibition assay. For the PNK inhibition assay, $(NH_4)_2SO_4$ and ADP were used as the model inhibitors. Various concentrations of inhibitors were added to the PNK reaction solution with a fixed concentration of PNK (1 U/mL). The procedures for the measurement of Cy5 counts were same as those of PKA assay described in main text. The relative activity (*RA*) of PKA was calculated based on equation 4.

$$RA = \frac{C_i}{C_t} \times 100\ \% = 10^{(N_i - N_t)/93.85} \times 100\ \% \qquad (4)$$

where N_t represents the Cy5 counts in the presence of 1 U/mL PNK, and N_i represents the Cy5 counts in the presence of 1 U/mL PNK + inhibitors. C_i and C_t were obtained according to the linear correlation equation (Fig. S8B), respectively.

$$N_t = 455.41 + 93.85 log_{10} C_t \qquad (5)$$

$$N_i = 455.41 + 93.85 log_{10} C_i \qquad (6)$$

The IC_{50} value of inhibitor was obtained from the curve-fitting equation (Fig. S10).

Cell culture and preparation of cell extracts for in vivo PNK assay. HeLa cells were cultured in Dulbecco's modified Eagle's medium (DMEM) supplemented with 10% fetal bovine serum (FBS)

and 1% penicillin-streptomycin at 37 ºC in a humidified atmosphere containing 5% CO_2. The cell counts were measured by Countstar automated cell counter (IC1000, Wilmington, DE, USA). Then the cell lysates were prepared using a nucleoprotein extraction kit (Sangon Biotech, Shanghai, China) according to the manufacturer's protocol. The collected cell lysates were used for PNK activity assay immediately or stored at −80 °C until use.

RESULTS AND DISCUSSION

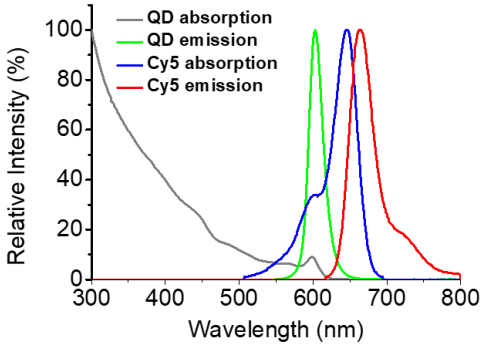

Fig. S1 Normalized absorption and emission spectra of the 605 nm-emission QD and Cy5. Gray line, absorption spectrum of the QD; Green line, emission spectrum of the QD; blue line, absorption spectrum of Cy5; Red line, emission spectrum of Cy5. The QD/Cy5 as a FRET pair permits only minimal spectral cross-talk. The broad absorption spectrum of the QD allows its excitation at 405 nm, which is near zero absorption of Cy5, efficiently eliminating direct acceptor excitation. Thus, the wavelength of 405 nm is chosen as the excitation light.

Calculation of the distance between the peptide-phosphate group and the DNA-phosphate group. The total length of -PO_3^{2-}-Zr^{4+}- PO_3^{2-}- structure was estimated by theoretical calculation with density functional theory (DFT). We used a computational model containing the Zr^{4+} and the adjacent amino acids (Ala-Ser-Leu) and deoxyribonucleotide (5'-deoxythymidine) which linked to Zr^{4+}. Geometries of the model system were optimized at the PCM/B3LYP level with 6-31G(d) basis set for nonmetal atoms.[1-3] The effective core potential ECP28MDF from the Stuttgart/Cologne group was adopted for Zr to approximate the relativistic effects.[4] The optimized geometries show that the distance between the peptide-phosphate group and the DNA-phosphate group is 4.64 Å with the P=O bond on the same side, and is 5.34 Å with the P=O bond on the opposite side.

Influence of the concentrations of PKA-induced phosphorylated peptide probe upon the assay performance. The various concentrations of PKA-induced phosphorylated peptide probes were mixed with 1 nM QDs, and the fluorescence intensities of both the QDs and Cy5 at the excitation wavelength of 488 nm were measured. As shown in Fig. S2, the value of F-F_0 enhances with the increasing concentrations of PKA-induced phosphorylated peptide probes from 250 nM to 1250 nM (F is the Cy5 fluorescence intensity in the presence of PKA, and F_0 is the Cy5 fluorescence intensity in the absence of PKA), and levels off beyond 1000nM.

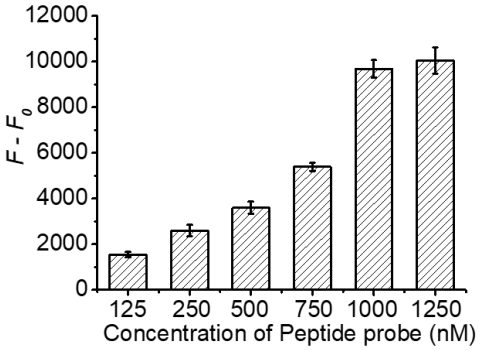

Fig. S2 Variance of F-F_0 value with the increasing concentrations of peptide probe. Error bars show the standard deviations of three independent experiments. The QD concentration is 1 nM.

Calibration curve between Cy5 fluorescence intensity and the concentration of peptide substrate. In 50 μL of reaction system, we measured the Cy5 fluorescence intensity in response to different concentrations of peptide probe (1, 10, 50 and 100 nM) using FLS-1000 fluorescence spectrometer with an excitation wavelength of 630 nm. The emission spectra were scanned from 645 nm to 750 nm, and the emission intensity at 667 nm (the maximum emission of Cy5) was used for data analysis. As shown in Fig. S3A, Cy5 fluorescence intensity enhances with the increasing concentration of peptide probe from 0 to 100 nM. The fitting equation is $F = 84.54 + 63.24\ C$ (R^2 =

0.9948), where *F* represents the Cy5 fluorescence intensity and *C* represents the concentration of peptide probe (nM).

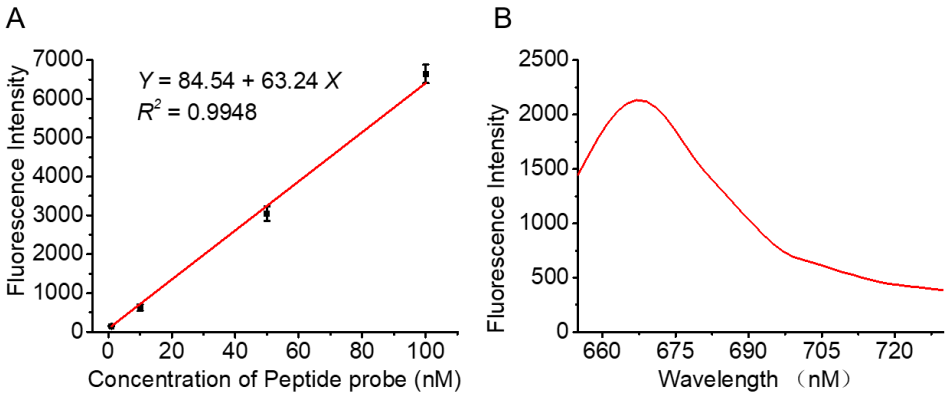

Fig. S3 (A) Calibration curve between Cy5 fluorescence intensity and the peptide probe concentration. Error bars show the standard deviation of three independent experiments. (B) Fluorescence emission spectra of the released Cy5 molecules from the streptavidin-coated magnetic beads.

Calculation of the ratio of Cy5-labeled peptide substrate to QD. We used fluorescence emission spectra to measure the number of Cy5-labeled peptide probe per QD. First, 18 μL of streptavidin-coated magnetic beads (MBs) solution (10 mg/mL) was added to the centrifuge tube and washed twice with 1× PBS buffer (pH 7.4). After magnetic separation, the supernatants were removed, and then the MBs were resuspended to 18 μL. Second, 18 μL of resultant MBs solution was mixed with 30 μL of capture probe (1 μM) and 152 μL of 1× PBS buffer (pH 7.4), followed by incubation at room temperature for 20 min. To remove the unconjugated substrates, the mixture was further magnetically separated, followed by washing three times with 1× PBS buffer (pH 7.4). Third, the mixture was resuspended to a total volume of 200 μL with 1× PBS buffer (pH 7.4). Fourth, we added 1.8 μL of 1 mM Zr^{4+} to the 20 μL of MB-conjugated substrates to form a mixture (30 μL), and then

incubated at room temperature for 1 h. Fifth, the reaction products of PKA-catalyzed phosphorylation were added to the mixture at room temperature, followed by incubation for 1 h. To remove the unconjugated substrates, the reaction products (50 μL) were further magnetically separated, followed by washing three times with 1× PBS buffer (pH 7.4). Then the mixture was resuspended to a total volume of 50 μL with 1× PBS buffer (pH 7.4). Sixth, capture probe and peptide probe were released from the MBs according to the instructions. Finally, the fluorescence intensity of the supernatant solution containing the released Cy5 molecules was measured by using FLS-1000 fluorescence spectrometer with an excitation wavelength of 630 nm. Fig. S3B shows the fluorescence emission spectra of the released Cy5 molecules from the streptavidin-coated magnetic beads. The concentration of Cy5 released from the magnetic beads is estimated to be 32.26 nM according to the calibration curve in Fig. S4A. The average number of Cy5 molecules per QD is calculated to be 32.26 nM / 1 nM = 32.

Optimization of experimental conditions for PKA assay. To achieve the best assay performance, we optimized the concentration of ATP, the reaction time of PKA, the concentration of Zr^{4+}, and the concentration of capture probe. We studied the effect of ATP concentration on the peptide phosphorylation efficiency. As shown in Fig. S4A, the value of F-F_0 enhances with the increasing concentration of ATP from 2.5 μM to 10 μM, followed by decrease beyond 10 μM. Thus, 10 μM is used as the optimal concentration of ATP in the further experiments. Another key factor to affect the peptide phosphorylation efficiency is the reaction time of PKA-induced phosphorylation of peptide probe. As shown in Fig. S4B, the value of F-F_0 enhances with the incubation time from 0.5 to 2.5 h, and levels off beyond 2 h. This can be explained by either the complete loss of PKA activity or the consumption of all available substrates. Thus, 2 h is selected as the optimal PKA reaction time

in the further experiments.

The concentrations of Zr^{4+} and capture probe are two important factors that influence the assay performance. As shown in Fig. S4C, the value of F-F_0 enhances with the increasing concentration of Zr^{4+} from 15 to 60 μM, followed by decrease beyond 60 μM. Thus, 60 μM Zr^{4+} is used in the subsequent experiments. We further optimized the concentration of capture probe. As shown in Fig. S4D, the value of F-F_0 enhances with the increasing concentration from 105 nM to 150 nM, and levels off beyond 150 nM. Thus, 150 nM capture probe is used in the subsequent experiments.

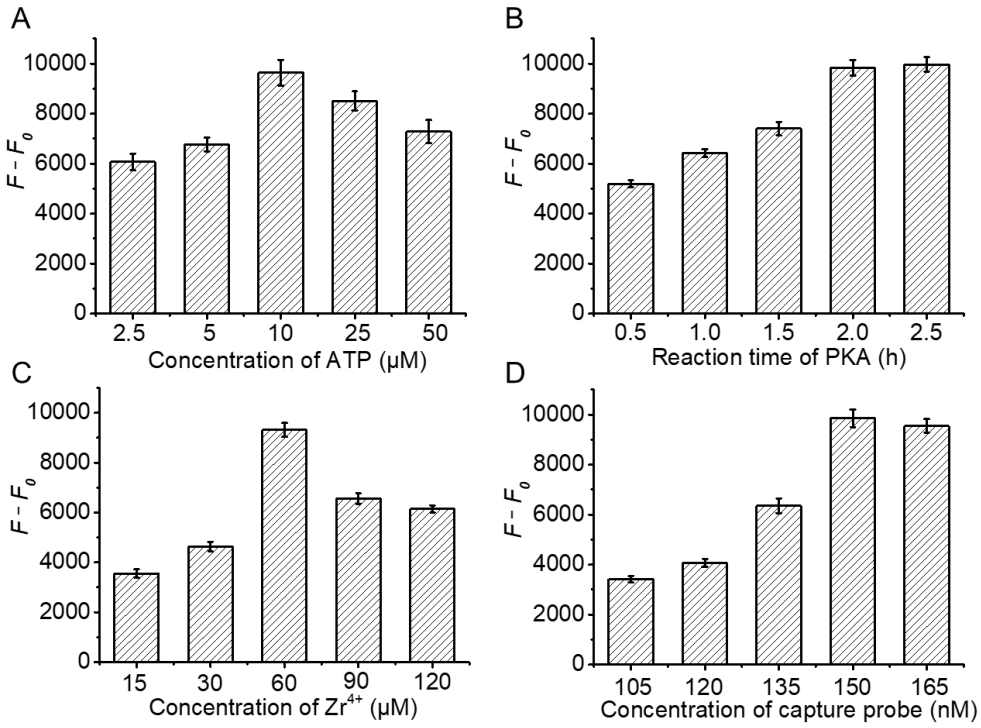

Fig. S4 (A) Variance of $F-F_0$ value with the different concentrations of ATP. (B) Variance of $F-F_0$ value in response to PKA reaction time. (C) Variance of $F-F_0$ value with the different concentrations of Zr^{4+}. (D) Variance of $F-F_0$ value with the different concentrations of capture probe. Error bars show the standard deviations of three independent experiments.

Detection of PNK Activity. To demonstrate the generality of this nanosensor, we employed it to

measure the PNK activity. We designed a Cy5 labeled-DNA (DNA probe, Fig. S5) for PNK assay. When PNK is present, it can catalyze the transfering of γ-phosphate group from ATP to 5′-hydroxyl group of oligonucleotidess, generating the phosphorylated DNA probe. With the assistance of Zr^{4+}, phosphorylated DNA probe can be attached to the QD−capture probe nanostructure via -PO_3^{2-}-Zr^{4+}-PO_3^{2-}- interaction to obtain a QD-Zr^{4+}-Cy5 nanostructure, leading to efficient FRET from the QD to Cy5. The resultant Cy5 signal can be simply measured by single-molecule detection. When PNK is absent, neither the phosphorylation of DNA probe nor the assembly of Cy5 onto a single QD can occur. Thus, no FRET signal can be detected.

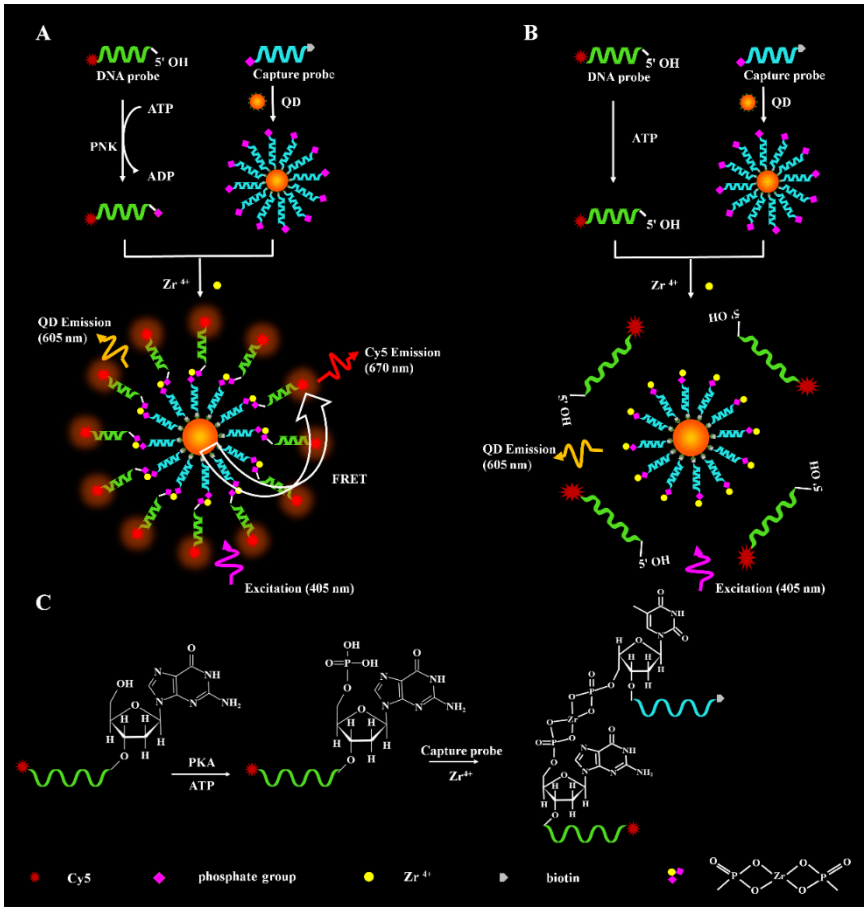

Fig. S5 (A) Schematic illustration of the Zr^{4+}-mediated assembly of single QD-based nanosensor for PNK assay. (B) No occurrence of FRET between the QD and Cy5 in the absence of PNK. (C) Mechanism of the unique coordinative interaction between Zr^{4+} and phosphorylated site of PNK-

produced phosphorylated DNA probes.

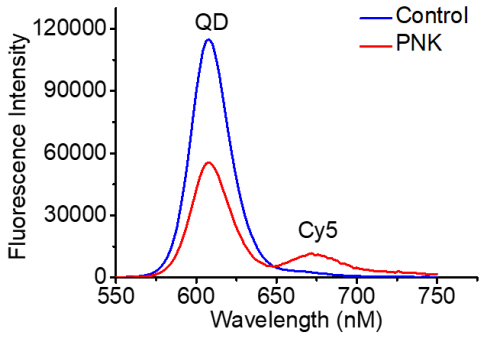

Fig. S6 Measurement of QD and Cy5 fluorescence emission spectra in the absence (control, blue line) and presence (red line) of PNK. The QD concentration is 1 nM, and the PNK concentration is 10 U /mL.

Validation of the proposed nanosensor for PNK assay. We demonstrated the feasibility of the proposed nanosensor for PNK assay by measuring fluorescence emission spectra (Fig. S6). In the absence of PNK, no Cy5 signal can be detected (Fig. S6, blue line), suggesting that no QD-Zr^{4+}-Cy5 nanostructure can be obtained. When PNK is present, a distinct Cy5 fluorescence signal is detected, accompanied by the decrease of QD fluorescence signal (Fig. S6, red line). The PNK activity was further measured by single-molecule detection (Fig. S7). When PNK is absent, only the QD fluorescence signals can be detected (Fig. S7A, green color), without Cy5 fluorescence signal being observed (Fig. S7B), indicating that FRET cannot occur without PNK. In contrast, when PNK is present, the fluorescence signals of both QDs (Fig. S7D, green color) and Cy5 (Fig. S7E, red color) can be simultaneously observed with perfect colocalization of both QD and Cy5 signals (Fig. S7F, yellow color), indicating the efficient FRET between QD and Cy5 induced by PNK.

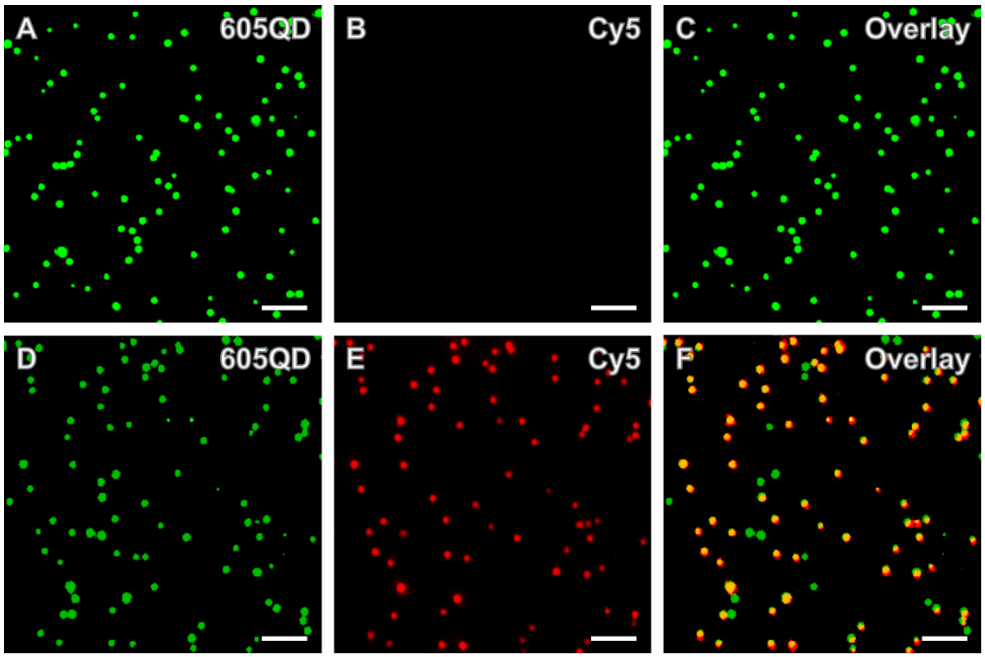

Fig. S7 Single-molecule fluorescence images in the absence (A−C) and presence of PNK (D−F). The signal of QD, Cy5, and colocalization is shown in green, red, and yellow, respectively. The PNK concentration is 10 U /mL. The scale bar is 3 μm.

Detection sensitivity of PNK assay. We investigated the sensitivity of the proposed nanosensor for PNK assay. When the concentration of PNK increases from 0.0001 to 10 U/mL, the Cy5 counts enhance correspondingly (Fig. S8A). The Cy5 counts show a linear correlation with the logarithm of PKA concentration in the range from 0.0001 to 0.03 U/mL (Fig. S7A). The correlation equation is $N = 455.41 + 93.85 \log_{10} C$ ($R^2 = 0.9956$), where N is the number of Cy5 counts and C is the concentration of PNK (U/mL). The limit of detection is calculated to be 1.40×10^{-5} U/mL by evaluating the control group plus three times standard deviation. The sensitivity of this method was enhanced by as much as 2 orders of magnitude compared with that of the smart three-dimensional (3D) DNA walking machine-based fluorescence method (0.0067 U/mL)[5] and 2 orders of magnitude compared with that of the ratio fluorescence method (0.0037 U/mL).[6] These results clearly

demonstrate the high sensitivity of the proposed nanosensor for PNK assay.

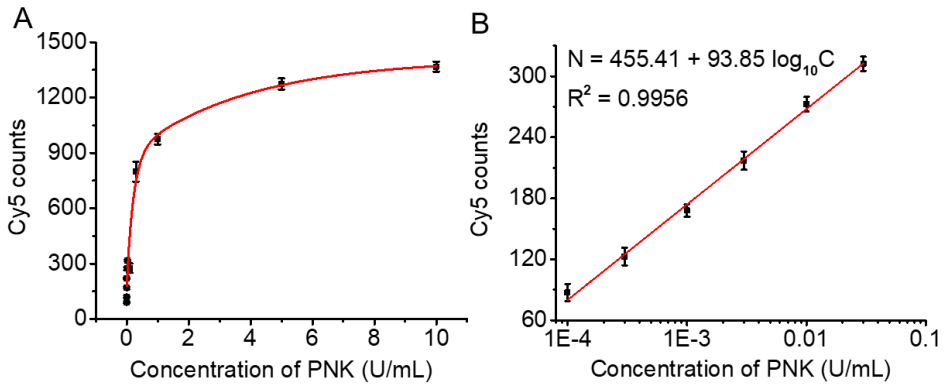

Fig. S8 (A) Measurement of Cy5 counts in response to different concentrations of PNK. (B) Linear relationship between Cy5 counts and the logarithm of PNK concentration in the range from 0.0001 to 0.03 U/mL. Error bars represent standard deviations of three experiments.

Detection selectivity of PNK assay. We used bovine serum albumin (BSA), immunoglobulin G (IgG), PKA, and uracil DNA glycosylase (UDG) as the nonspecific proteins. As shown in Fig. S9, in the presence of nonspecific proteins, no significant Cy5 signal is observed, suggesting no occurrence of FRET between QD and Cy5. In contrast, in the presence of PNK, high Cy5 signal can be observed, indicating the efficient FRET between QD and Cy5. These results clearly demonstrate the high specificity of the proposed method for PNK assay.

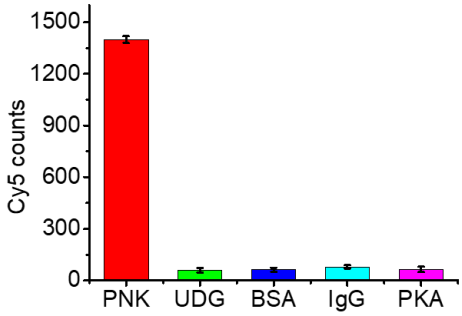

Fig. S9 Cy5 counts in response to 100 U/mL PKA (red color), 100 U/mL UDG (green color), 10

U/mL PNK (magenta color), 0.005 g/L IgG (cyan color), and 0.005 g/L BSA (blue color), respectively. Error bars represent standard deviations of three experiments.

PNK Inhibition Assay. We employed the proposed nanosensor for PNK inhibitor assay. The ADP is the byproduct of the PNK-catalyzed phosphorylation reaction, and it can severely inhibit PNK activity because the coexistence of ADP and 5'-phosphorylated DNA can reverse the phosphorylation reaction.[7] In addition, high-concentration salts (e.g., $(NH_4)_2SO_4$) may induce the conformational change of PNK enzyme,[8] and efficiently inhibit the PNK activity. The relative activity of PNK decreases with the increasing concentration of ADP (Fig. S10A) and $(NH_4)_2SO_4$ (Fig. S10B), respectively. The IC_{50} values are calculated to be 0.24 mM for ADP and 5.11 mM for $(NH_4)_2SO_4$, respectively, consistent with those obtained by the molecular beacon-based fluorescent assay (0.8 mM for ADP)[8] and the bioluminescent assay (9.88 mM for $(NH_4)_2SO_4$)[9]. These results suggest that the proposed nanosensor can be used to screen the PNK inhibitors, holding great potential in drug discovery.

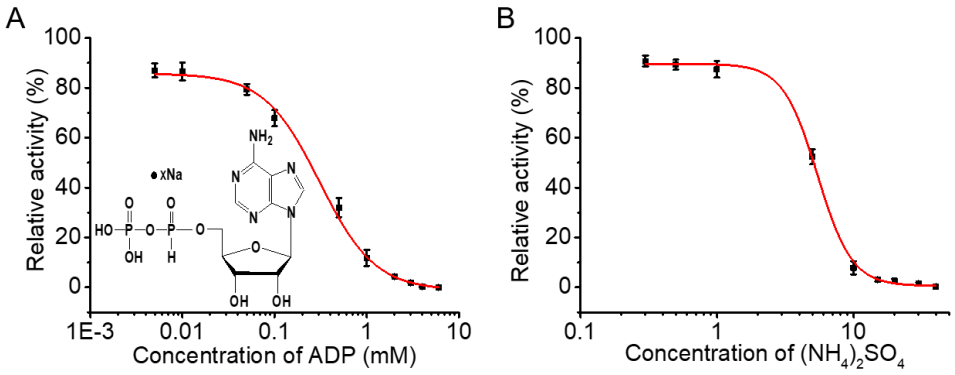

Fig. S10 (A) Inhibition effect of ADP upon the PNK activity. (B) Inhibition effect of $(NH_4)_2SO_4$ upon the PNK activity. Error bars represent standard deviations of three experiments.

PNK kinetic analysis. We employed this nanosensor to monitor the phosphorylation reaction in response to various concentrations of DNA substrate. For kinetic analysis, we measured Cy5 counts in response of variable reaction time of PNK from 0.25 h to 2 h. The Cy5 counts enhance with reaction time (Fig. S11A). The initial velocity was measured in the presence of 10 U/mL PNK and various concentrations of DNA substrate in 10-min reaction at 37°C to make sure that ~80% of the substrates were unconsumed (i.e., in the initial-rate regime). Fig. S10B shows that the initial velocity of PNK enhances with the increasing concentration of DNA probe. We fit the experimental data to the Michaelis−Menten equation $V = V_{max}\ [\mathrm{S}]/(K_m + [\mathrm{S}])$, where V_{max} is the maximum initial velocity, and $[S]$ is the DNA substrate concentration, and K_m is the Michaelis−Menten constant corresponding to the concentration at half-maximal velocity. The V_{max} is evaluated to be 37.76 min^{-1}, and K_m is calculated to be 0.77 μM. The K_m value is consistent with that obtained by using a fluorophore-labeled DNA-hairpin smart probe (0.56 μM),[10] suggesting that the proposed nanosensor can be used to accurately evaluate the kinetic parameters of PNK.

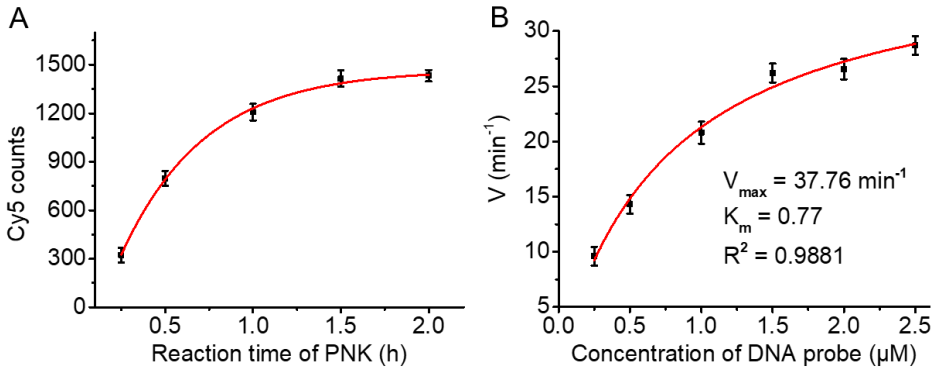

Fig. S11 (A) Measurement of Cy5 counts in response to reaction time of PNK. (B) Variance of initial velocity (V) with various concentrations of DNA substrates. The PNK concentration is 10 U/mL. Error bars represent standard deviations of three experiments.

Detection of PNK from cell extracts. We measured the PNK activity of the extracted nucleoprotein in Hela cells. In the logarithmic scale, the Cy5 counts exhibits a linear correlation with the cell number in the range of 1 – 1000 cells (Fig. S12). The regression equation is $N = -122.12 + 323.93 \log_{10} X$, with a correlation coefficient (R^2) of 0.9959, where X is the cell number. The limit of detection is calculated to be 3 cells by evaluating the control group plus three times standard deviation.

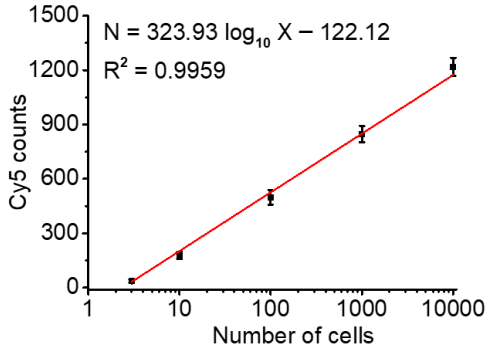

Fig. S12 Linear relationship between the Cy5 counts and the logarithm of HeLa cell number in the range of 3 – 10000 cells. Error bars represent standard deviations of three experiments.

References

1. (a) C. Lee, W. Yang and R. G. Parr, Phys Rev B Condens Matter, 1988, 37, 785-789; (b) A. D. Becke, The Journal of Chemical Physics, 1993, 98, 5648-5652; (c) B. M. J. Tomasi, J. Chem. Phys., 1997, 106, 5151–5158.

2. K. A. Peterson, D. Figgen, M. Dolg and H. Stoll, J. Chem. Phys., 2007, 126, 124101.

3. C. Feng, Z. Wang, T. Chen, X. Chen, D. Mao, J. Zhao and G. Li, Anal. Chem., 2018, 90, 2810-2815.

4. M. Wang, D. Kong, D. Su, Y. Liu and X. Su, Nanoscale, 2019, 11, 13903-13908.

5. Z. Tang, K. Wang, W. Tan, C. Ma, J. Li, L. Liu, Q. Guo and X. Meng, Nucleic Acids Res., 2005, 33, e97.

6. T. Hou, X. Wang, X. Liu, T. Lu, S. Liu and F. Li, Anal. Chem., 2014, 86, 884-890.

7. J. Du, Q. Xu, X. Lu and C. Y. Zhang, Anal. Chem., 2014, 86, 8481-8488.

8. C. Song and M. Zhao, Anal. Chem., 2009, 81, 1383-1388.